



# Protein-based carbon and platinum nanocomposites as electrocatalysts for methanol oxidation activity

Young-Geun Lee <sup>a,1</sup>, Geon-Hyoung An <sup>b,1</sup>, Hyo-Jin Ahn <sup>a,b,\*</sup>

<sup>a</sup> Department of Materials Science and Engineering, Seoul National University of Science and Technology, Seoul 139-743, North Korea

<sup>b</sup> Program of Materials Science & Engineering, Convergence Institute of Biomedical Engineering and Biomaterials, Seoul National University of Science and Technology, Seoul 139-743, North Korea

## ARTICLE INFO

### Article history:

Received 11 January 2018

Received in revised form

28 March 2018

Accepted 6 April 2018

Available online 11 April 2018

### Keywords:

Methanol oxidation

Pt electrocatalysts

Protein based carbon

Nitrogen doping

High electrochemical performance

## ABSTRACT

Owing to the characteristics of high energy density, low operating temperature, and environmentally-friendly features, direct methanol fuel cells (DMFCs) are a promising renewable energy source. However, the electrocatalysts of the anode are vulnerable in terms of their electrochemical performance, as they can be easily toxified by CO and other hydrocarbons, which might lead to a break-up of the methanol oxidation reaction (MOR). For further advances in the DMFC industry with improved electrochemical performance, this issue should be urgently resolved. Thus, this study proposes a novel approach to synthesize protein-based carbon as platinum electrocatalyst supports (PCPs) from tofu using a carbonization for the improved methanol oxidation activities. Among commercial Pt/C and other samples, the composite loaded 10 wt% Pt electrocatalyst showed the highest anodic current density of 510 mA mg<sub>Pt</sub><sup>-1</sup>, the excellent electrocatalytic stability, and the highest retention of 86%. The improved electrochemical performances can be attributed to the good dispersion of Pt electrocatalysts and N-doping effect of protein-based carbon supports. These results suggest that PCPs derived from tofu will be one of promising candidates as platinum catalyst supports to improve methanol oxidation activities.

© 2018 Elsevier B.V. All rights reserved.

## 1. Introduction

In recent years, the development of renewable power resources has become a key issue on the way towards realizing the global object of reducing consumption of fossil fuels and moving to new clean energy technologies. Due to their low operating temperature, high energy conversion, high energy density, and low emission of pollutants, direct methanol fuel cells (DMFCs) are nowadays a promising renewable energy source for airport baggage trucks, smaller boats, and torches [1–5]. The four main components of DMFCs include the anode, cathode, membrane, and electrolyte. During the operation, methanol oxidation reaction (MOR,  $\text{CH}_3\text{OH} + \text{H}_2\text{O} \rightarrow \text{CO}_2 + 6\text{H}^+ + 6\text{e}^-$ ) occurs on the electrocatalysts of the anode that define the electrochemical performance and cost-effectiveness of DMFCs [6–10]. However, a weak point of DMFCs is that they mainly employ Pt electrocatalysts, which might lead to

several important disadvantages, such as the high cost of Pt, inclination to agglomerate of Pt, and poor CO tolerance arising due to the accumulation of surface-adsorbed intermediate species, such as CO, CHO, and COOH. Among them, the use of high-priced Pt is the most significant challenge that hinders the industrial use of DMFCs [11–15].

To solve these problems, previous studies have sought to find strategies to enhance the efficiency of Pt electrocatalysts, such as the controlling the morphology, the introduction of support materials, and alloying them with various metals [16–18]. The introduction of support materials, such as metal/metal oxide, carbide, and carbon, is among the most promising strategies to minimize the loading of Pt electrocatalysts and enhance their electrochemical performance in DMFCs. In general, the latest DMFCs technology uses various carbon-based supports, such as graphite, carbon nanotubes, and carbon nanofiber, characterized by high electrical conductivity, excellent electrocatalytic stability, and high surface area [19–22]. However, to expand the DMFC industry, it is necessary to provide a better performance than the existing carbon supports.

Therefore, in the present study, we used a new carbon with

\* Corresponding author. Department of Materials Science and Engineering, Seoul National University of Science and Technology, Seoul 139-743, North Korea.

E-mail address: [hjahn@seoultech.ac.kr](mailto:hjahn@seoultech.ac.kr) (H.-J. Ahn).

<sup>1</sup> Y.-G. Lee and G.-H. An. contributed equally to this work.

protein for Pt electrocatalyst supports. Overall, while several oil- and biomass-based carbons for Pt electrocatalyst supports have been investigated to date, no research has been conducted on protein-based carbons. Accordingly, in the present study, we focused on proteins from tofu for Pt electrocatalyst supports. Tofu is a traditional Asian food consisting of 80 wt% water and 20 wt% protein. High protein content and few impurities makes it suitable for the use as a precursor of carbon [23–25]. In addition, since the amino acid constituting the protein contains nitrogen, N-doped carbon can be produced simultaneously. Recently, several studies demonstrated that heteroatoms doped carbon supports, particularly nitrogen, can improve the physical and electrochemical properties. The affluent free  $\pi$  electrons, inert for chemical reactions, are available in the carbon, making it a potential electrocatalyst material. The carbon  $\pi$  electrons can be activated because it conjoins with long-pair electrons from nitrogen dopants. In addition, it was found that the existence of N-doping can also introduce a chemically active site on the carbon support that acts as an anchoring site for Pt nanoparticles deposited on its surface with the synergistic interaction of Pt electrocatalyst and carbon support [25,26]. Therefore, these advantages of N-doped carbon derived from tofu can provide improved electrocatalytic activity and stability.

In the present study, we successfully fabricated protein-based carbon as Pt electrocatalysts supports and controlled the amount of platinum loading for the optimal electrocatalysts for the methanol oxidation activities.

## 2. Experimental

### 2.1. Chemicals

The tofu was purchased from Pulmuone Co., Ltd. (Korea). The chloro-platinic acid hydrate ( $\text{H}_2\text{PtCl}_6 \cdot x\text{H}_2\text{O}$ ,  $\geq 99.9\%$ ), sodium boron-hydride ( $\text{NaBH}_4$ ), 2-propanol, Nafion perfluorinated resin solution, methanol (anhydrous, 99.8%), hydrofluoric acid (HF, ACS reagent, 52%), nitric acid ( $\text{HNO}_3$  ACS reagent 66%), and sulfuric acid ( $\text{H}_2\text{SO}_4$ , ACS reagent, 70%) were obtained from Sigma-Aldrich. All chemicals were used without further purification.

### 2.2. Synthesis of protein-based carbon as platinum electrocatalysts supports

The protein-based carbon as Pt electrocatalysts supports were prepared by the carbonization. Firstly, the tofu was dried in an oven at 80 °C to eliminate any moisture, then heated at 300 °C to remove impurities, and, finally, carbonized at 800 °C for 2 h under the nitrogen atmosphere. The carbonized sample was acid-treated using a mixture (1:1 (v/v)) of HF and  $\text{HNO}_3$  to form the functional groups on the surface. Thereafter, the ball mill was employed to obtain the nano-sized support. To fabricate the Pt electrocatalysts on the supports, the reduction method was used. The N-doped carbon support was dispersed in 0.14 mM, 0.28 mM, and 0.56 mM  $\text{H}_2\text{PtCl}_6 \cdot x\text{H}_2\text{O}$  ( $\geq 99.9\%$ ) solution in deionized (DI) water and reduced by  $\text{NaBH}_4$  to load 5, 10, and 20 wt% Pt electrocatalyst on the support, respectively. The obtained samples were washed several times in DI water and then freeze-dried at –50 °C to get the metallic Pt phases. Therefore, we successfully obtained the protein-based carbon as 5, 10, and 20 wt% Pt electrocatalysts supports (herein referred to as PCP-5, PCP-10, and PCP-20). The conventional Pt/C (20 wt% Pt on Vulcan carbon, De Nora S.P.A.) was used for comparison.

### 2.3. Characterization

The morphologies and structures of the samples were examined using field emission–scanning electron microscopy (FE-SEM, Hitachi S–4800) and transmission electron microscopy (MULTI/TEM; Tecnai G<sup>2</sup>, KBSI Gwangju Center). The crystal structures and chemical bonding states of the samples were characterized by X-ray diffractometry (XRD, Rigaku D/Max 2500 V) with the Cu  $K_\alpha$  radiation in the range from 10° to 90° with the step size of 0.02° and X-ray photoelectron spectroscopy (XPS, ESCALAB 250) with an Al  $K_\alpha$  X-ray source. The binding energies of the XPS spectra were standardized to the C 1s core level (284.5 eV).

### 2.4. Electrochemical characterization

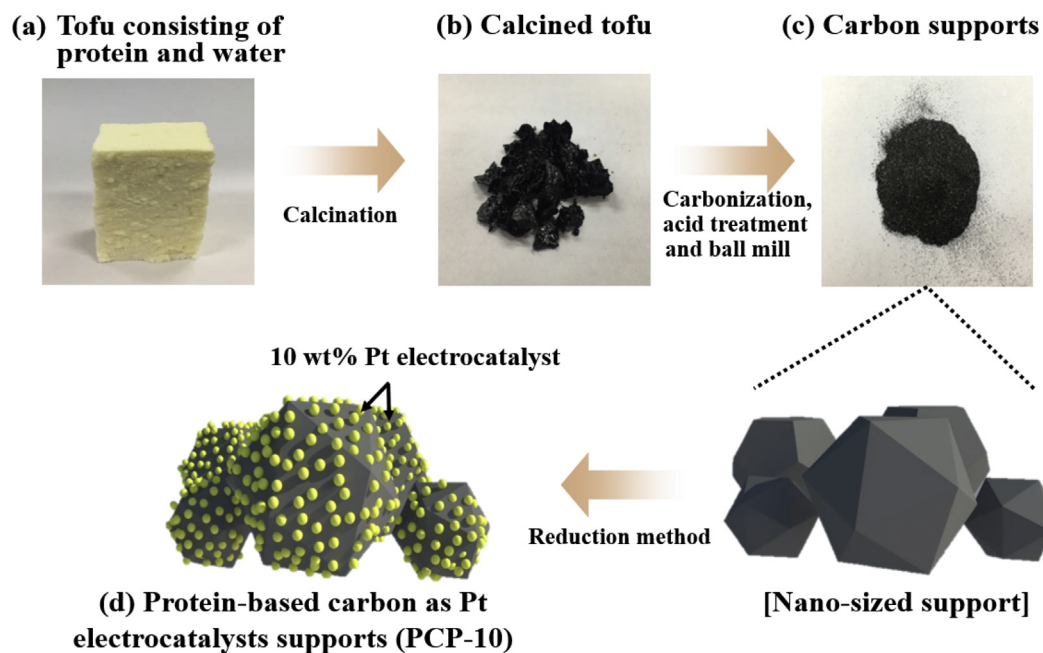
Electrochemical performance measurements were performed using a potentiostat/galvanostat (Ecochemie Autolab PGST302 N, Netherlands) in a conventional three-electrode system consisting of a the working electrode (glassy carbon electrode, area = 0.0706 cm<sup>2</sup>), the counter electrode (Pt gauze), and the reference electrode (Ag/AgCl, sat. KCl). To investigate the methanol oxidation activities, all samples were mixed to inks of 80 wt% electrocatalysts and 20 wt% Nafion in 2-propanol. All inks were then carefully dropped on the glassy carbon electrode and dried at 60 °C. In the next step, the methanol oxidation activity tests were run using cyclic voltammograms (CV) in a 2 M  $\text{CH}_3\text{OH}$  and 0.5 M  $\text{H}_2\text{SO}_4$  electrolyte between –0.2 and 1.0 V (vs. Ag/AgCl) at the scan rate of 50 mV s<sup>–1</sup>. To examine the electrocatalytic stability and retention, chrono-amperometry (CA) was performed in a 2 M  $\text{CH}_3\text{OH}$  and 0.5 M  $\text{H}_2\text{SO}_4$  electrolyte at the constant potential of 0.5 V for 2000s and 0.45 V for 7200s, respectively. For comparison, electrochemical performance measurements of commercial Pt/C were also performed under the same conditions.

## 3. Results and discussion

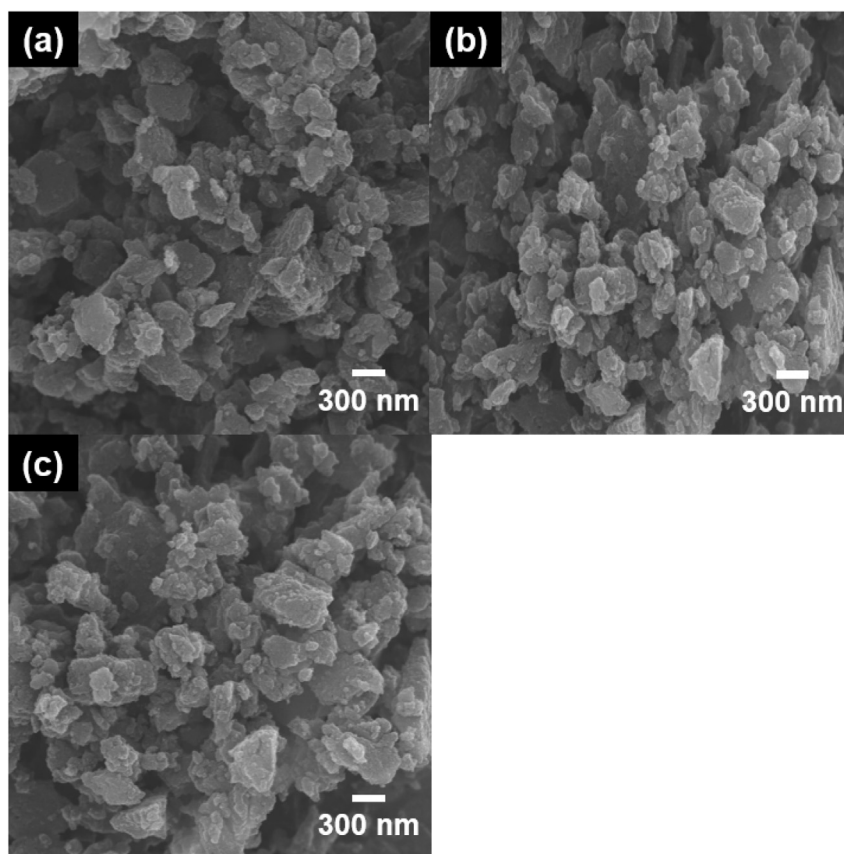
Fig. 1 illustrates the synthetic process for fabricating PCP-10. The tofu (see Fig. 1a) consisting of protein and water was dried to eliminate moisture and then heated at 300 °C to make calcined tofu (see Fig. 1b); therefore, tofu-based carbon supports were formed using ball mill and carbonization (see Fig. 1c). In addition, to form the functional group on the surface, we used acid treatment. Finally, PCP-10 (see Fig. 1d) was synthesized using the reduction method, implying that well-dispersed Pt electrocatalysts on the protein-based carbon were formed.

Fig. 2 shows the SEM images obtained from PCP-5, PCP-10, and PCP-20. The diameters of the samples amounted to ca. 254–311 nm for PCP-5, 221–315 nm for PCP-10, and 230–319 nm for PCP-20. All samples showed the semi-block morphology. To further examine the structural properties and morphological of the samples, TEM measurements were performed.

Fig. 3 shows low-resolution (Fig. 3a–c) and high-resolution (Fig. 3d–f) TEM images of PCP-5, PCP-10, and PCP-20. PCP-5 (see Fig. 3a and d) showed that Pt electrocatalysts were sparsely distributed on the protein-based carbon due to a small amount of Pt precursor when the reduction method was used. Among the samples, PCP-10 (Fig. 3b and e) exhibited an excellent dispersion of Pt electrocatalyst on the protein-based carbon and a relatively small amount of Pt agglomeration. In addition, PCP-10 indicated the nanosized Pt electrocatalyst particles (3–4 nm) and definite lattice fringes with the spacing of 0.22 nm, which were attributed to the (111) planes of Pt [3,22]. The excellent dispersion of nanosized Pt can provide the large electrochemical active sites, resulting in excellent electrocatalytic activity during the methanol oxidation. However, PCP-20 (see Fig. 3c and f) showed the agglomerated Pt



**Fig. 1.** Schematic illustration for the synthetic process of protein based carbon as a platinum catalysts supports (a) Tofu purchased from Pulmuone, (b) Calcined tofu, (c) Resultant carbon supports using carbonization ball mill, and acid treatment, (d) protein based carbon as a platinum catalysts supports using the reduction method.



**Fig. 2.** The SEM images of (a) PCP-5, (b) PCP-10, and (c) PCP-20.

electrocatalyst on the protein-based carbon owing to exceed loading of Pt precursor during a reduction method. The agglomerated Pt electrocatalyst could reduce the electrocatalytic activity

during the methanol oxidation due to the few electrochemical active sites. To further explain the distribution of C, N, and Pt atoms of PCP-10, the TEM-EDS mapping was performed (see Fig. 3g). The

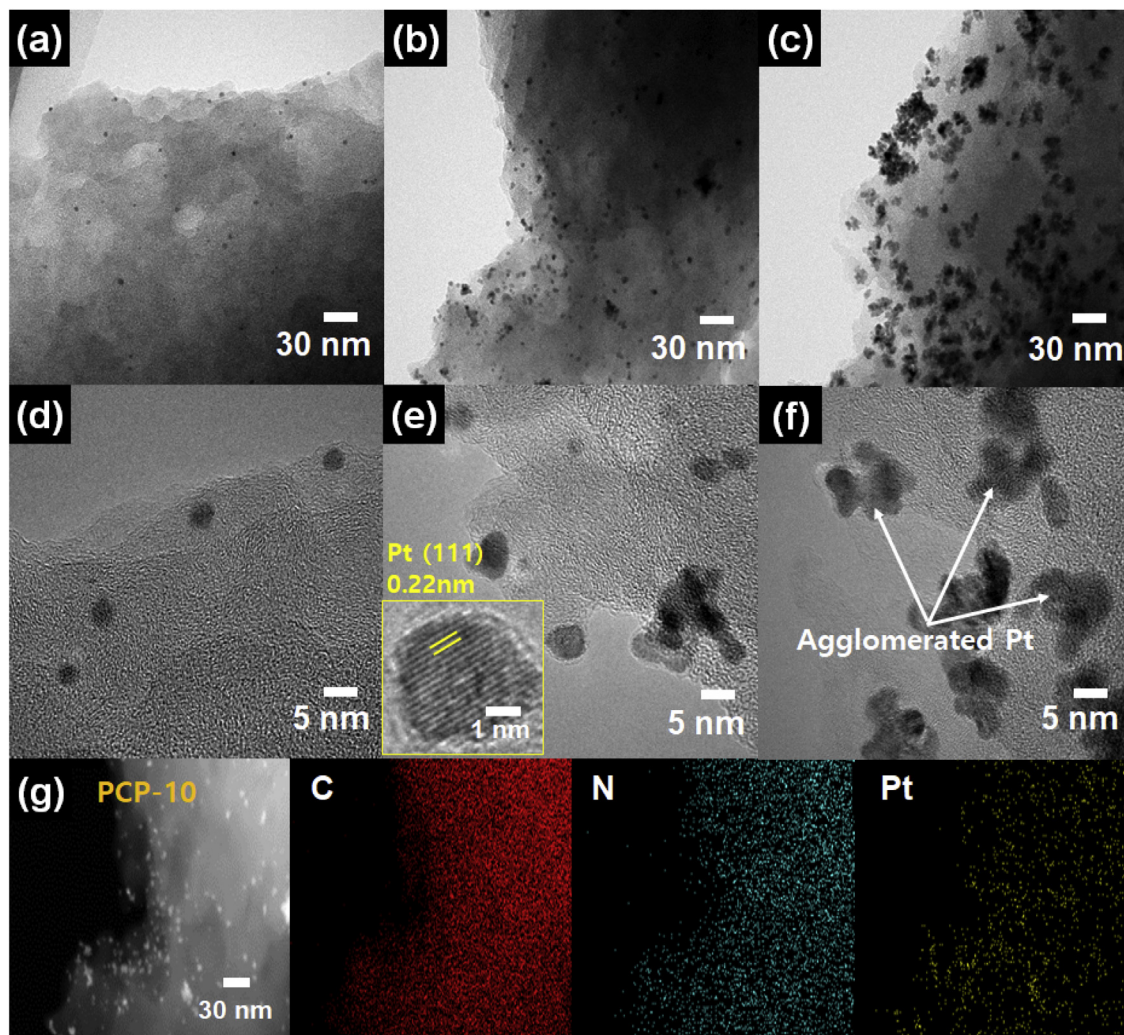


Fig. 3. (a–d) Low-resolution and (e–h) high-resolution TEM images of (a and d) PCP-5, (b and e) PCP-10, (c and f) PCP-20, and (g) TEM-EDS mapping data of PCP-10.

EDS results suggest that Pt atoms were uniformly distributed along the carbon, indicating a uniform fabrication of Pt electrocatalysts. In addition, due to the N-containing protein, the N atoms were uniformly dispersed.

Fig. 4a shows the XRD data of PCP-5, PCP-10, and PCP-20 to illustrate their crystal structure and crystalline phases. All of the samples exhibited a broad peak at around  $25^\circ$ , indicating the (002) layer of graphite, and the main diffraction peaks at  $39.7^\circ$ ,  $46.2^\circ$ ,  $67.5^\circ$ , and  $81.3^\circ$  corresponding to the (111), (200), (220), and (311) planes of the face-centered cubic Pt phases of the space group  $Fm\bar{3}m[225]$  (JCPDS card No. 04-0802), respectively [3,27]. Furthermore, the Scherrer equation was used to examine the particle size of the Pt electrocatalysts of PCP. The diffraction peaks of PCP were calculated by the Scherrer equation (see Eq. (1)) [21,28]:

$$D = 0.9\lambda / (\beta \cos\theta) \quad (1)$$

where  $\lambda$  is the X-ray wavelength,  $\beta$  is the full width at half maximum (FWHM), and  $\theta$  is the Bragg angle. The average sizes of Pt electrocatalysts were calculated using (111), (200), (220), and (311) planes. These calculated values amounted to  $\sim 3.6$  nm for PCP-5,  $\sim 3.5$  nm for PCP-10, and  $\sim 5.1$  nm for PCP-20, and were congruent with the measured TEM results. Based on SEM, TEM, and XRD results, it can be concluded that PCP-10 were successfully

synthesized. To demonstrate the chemical binding states of PCP-10, XPS measurements were performed. By using the C1s line (248.5 eV) as the reference for the charge collection, calibration on all spectral peaks was performed. Fig. 4b shows the Pt  $4f_{7/2}$  and Pt  $4f_{5/2}$  photoelectrons in the Pt 4f core-level spectra of PCP-10 with the peaks at 71.3 eV and 74.7 eV, respectively, corresponding to metallic Pt [18,21]. In addition, the second set of doublets envisaged at 72.3 eV and 75.4 eV was related to Pt species, such as PtO and Pt(OH)<sub>2</sub>, because of the oxidation of Pt by O<sub>2</sub> and water vapor in the air [3,22]. Furthermore, Fig. 4c shows N1s peaks in the XPS spectra of PCP-10. The four types of nitrogen in PCP-10 were in the form of pyridinic-N oxide ( $403.0 \pm 0.3$  eV), graphitic-N ( $401.0 \pm 0.3$  eV), pyrrolic-N ( $400.0 \pm 0.3$  eV), and pyridinic-N ( $398.4 \pm 0.3$  eV). Specifically, the pyridinic-N, which possesses a pair of electron in the plane of the carbon matrix, could offer one p-electron to the aromatic  $\pi$ -systems, which led to the augmentation of electron-donor property for electrocatalytic activity. Thus, the existence of pyridinic-N of carbon support resulted in a considerable enhancement of electrochemical performance [25,26,29]. Based on the SEM, TEM, TEM-EDS mapping, XRD, and XPS results, it can be concluded that PCP were successfully synthesized.

Next, to examine the electrocatalytic activities of the prepared samples, the CV measurement for the methanol oxidation activity was performed between  $-0.2$  and  $1.0$  V (vs. Ag/AgCl) at a  $50$  mV s<sup>-1</sup>

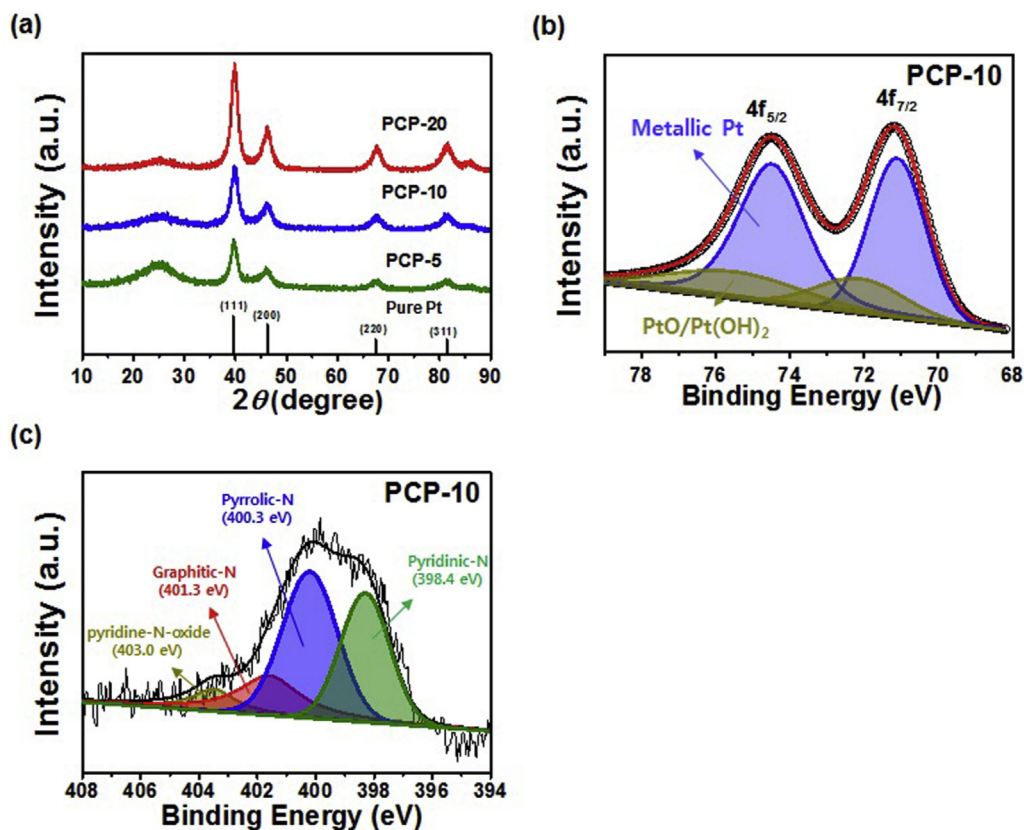


Fig. 4. (a) The XRD data of PCP-5, PCP-10, and PCP-20, (b and c) The XPS data of PCP-10 for Pt and nitrogen species, respectively.

in a 2 M CH<sub>3</sub>OH and 0.5 M H<sub>2</sub>SO<sub>4</sub> electrolyte (see Fig. 5b). The measured values were normalized by the Pt loading mass. In general, the methanol oxidation activity turned out 6 protons, 6 electrons, and carbon dioxide (CH<sub>3</sub>OH + H<sub>2</sub>O → 6e<sup>-</sup> + 6H<sup>+</sup> + CO<sub>2</sub>) [30].

The onset potential of methanol oxidation reaction can prove the electrocatalytic activity of the catalysts. As shown Fig. 5a, PCP-10 showed the lowest onset potential of 0.07 V, indicating that the optimum amount of Pt loading using the reduction method.

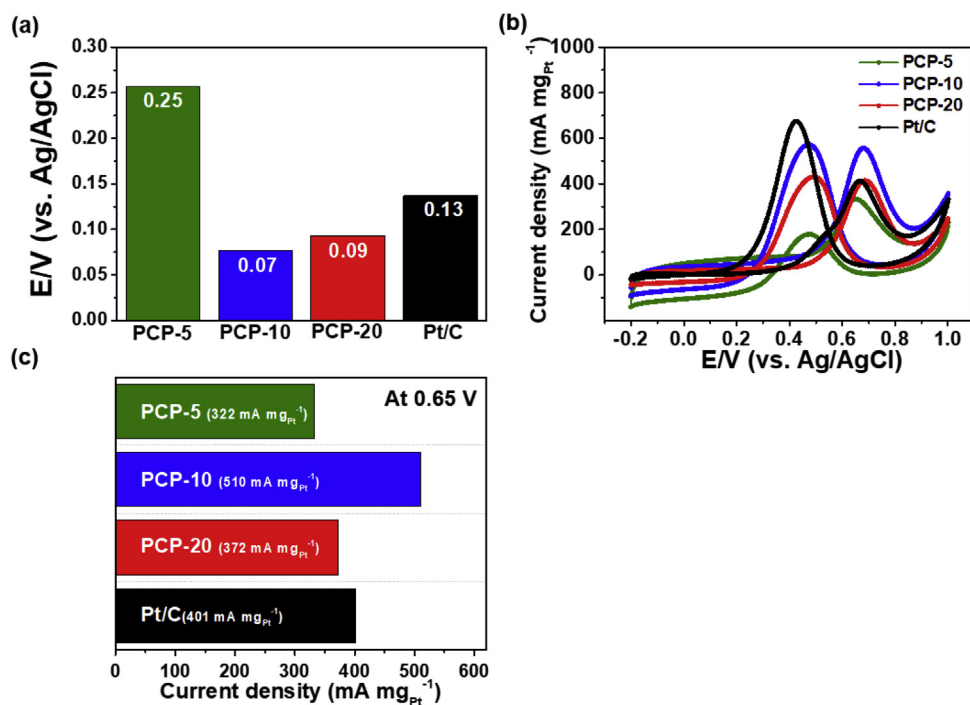


Fig. 5. Comparison of the electrocatalytic activity of PCP-5, PCP-10, PCP-20, and commercial Pt/C (a) On set potential in the forward scan, (b) Cyclic voltammetry (CV) measurements of methanol oxidation of PCP-5, PCP-10, PCP-20, and commercial Pt/C at the scan rate of 50 mV s<sup>-1</sup> in the voltage range of -0.2–1.0 V (c) Anodic current densities of all the samples at 0.65 V.

Furthermore, the CV curves (see Fig. 5b) of PCP-5, PCP-10, PCP-20, and Pt/C exhibited two peaks indicated as forward and backward peaks. These forward peak and the backward peak suggest anodic current density and intermediate species, such as CO, CHO, and COOH, respectively [12,19,22]. Thus, the anodic current density can be concluded to be directly related to the electrochemical performance of the methanol oxidation reaction corresponding to forward peaks. For the forward peaks of PCP-10, the more the number of electrons generated in the anode, the higher the anodic current density, implying an improved electrochemical performance of the methanol oxidation reaction. Fig. 5c shows that the anodic current densities of PCP-5, PCP-10, PCP-20, and commercial Pt/C were  $322 \text{ mA mg}_{\text{Pt}}^{-1}$ ,  $510 \text{ mA mg}_{\text{Pt}}^{-1}$ ,  $372 \text{ mA mg}_{\text{Pt}}^{-1}$ , and  $401 \text{ mA mg}_{\text{Pt}}^{-1}$  in the forward scan at 0.65 V, respectively. As shown in Fig. 5c, PCP-10 had the highest anodic current density of ca. 1.6, 1.4, and 1.3 times higher than the corresponding values of PCP-5, PCP-20, and commercial Pt/C, respectively. Therefore, the enhanced electrochemical activity of PCP-10 can be attributed to the well-dispersed Pt electrocatalysts, leading to large electrochemical active sites. In addition, the N-doping proved to be an efficient electron transport during the methanol oxidation reaction.

One of the key factors for DMFC development is the improvement of electrocatalytic stability. Accordingly, in order to examine electrocatalytic stability of all samples, CA test was performed at 0.5 V in a 2 M CH<sub>3</sub>OH and 0.5 M H<sub>2</sub>SO<sub>4</sub> electrolyte for 2000s (see Fig. 6a). The CV curves showed a quick current degradation during the initial stage due to the generation of intermediate species such as CHO<sub>ads</sub> and CH<sub>3</sub>OH<sub>ads</sub>, and adsorption of SO<sub>4</sub><sup>2-</sup> anion on the Pt electrocatalyst surface. This intermediate species and adsorption of SO<sub>4</sub><sup>2-</sup> anion on the Pt electrocatalyst obstructed the methanol oxidation activity [3,8,21]. Nevertheless, as compared to other samples, PCP-10 sustained the highest current density and the

lowest degradation rate during the methanol oxidation activity. Furthermore, to examine electrocatalytic retention, CA test was run at 0.45 V in a 2 M CH<sub>3</sub>OH and 0.5 M H<sub>2</sub>SO<sub>4</sub> electrolyte for 7200s; next, the CV test was performed between -0.2 and 1.0 V (vs. Ag/AgCl) at a 50 mV s<sup>-1</sup>. Fig. 6b–c shows the CV curves of PCP-10 and Pt/C after the CA test, respectively. PCP-10 displays the excellent retention of 86% compared to Pt/C (70%), as the introduction of N-doping would strengthen the relationship between Pt electrocatalyst and protein-based carbon supports, thus improving the structure stability of Pt electrocatalyst [31,32]. These results suggest that N-doping of protein-based carbon can effectively improve the electrocatalytic stability and retention owing to the synergistic interaction of Pt electrocatalyst and carbon support.

PCP-10 showed improved electrochemical performance in the methanol oxidation activity for the following two major reasons. First, since a good distribution of Pt electrocatalyst on the support offered an increased contact area between the Pt electrocatalyst and the electrolyte, the anodic current density increased during the methanol oxidation activity. Second, the existence of N-doping in the support was able to augment electron-donor property of Pt electrocatalyst and the synergistic interaction of Pt electrocatalyst and carbon support, leading to a higher enhancement of electrochemical performance. Therefore, due to its showing a combination of these two advantages, PCP-10 can be concluded to be a promising candidate as a novel support for high-performance DMFCs.

#### 4. Conclusions

In the present study, PCPs were successfully synthesized using the carbonization and the reduction methods. Specifically, as compared to PCP-5, PCP-20, and a commercial Pt/C, PCP-10 showed improved electrochemical performances with the lowest onset

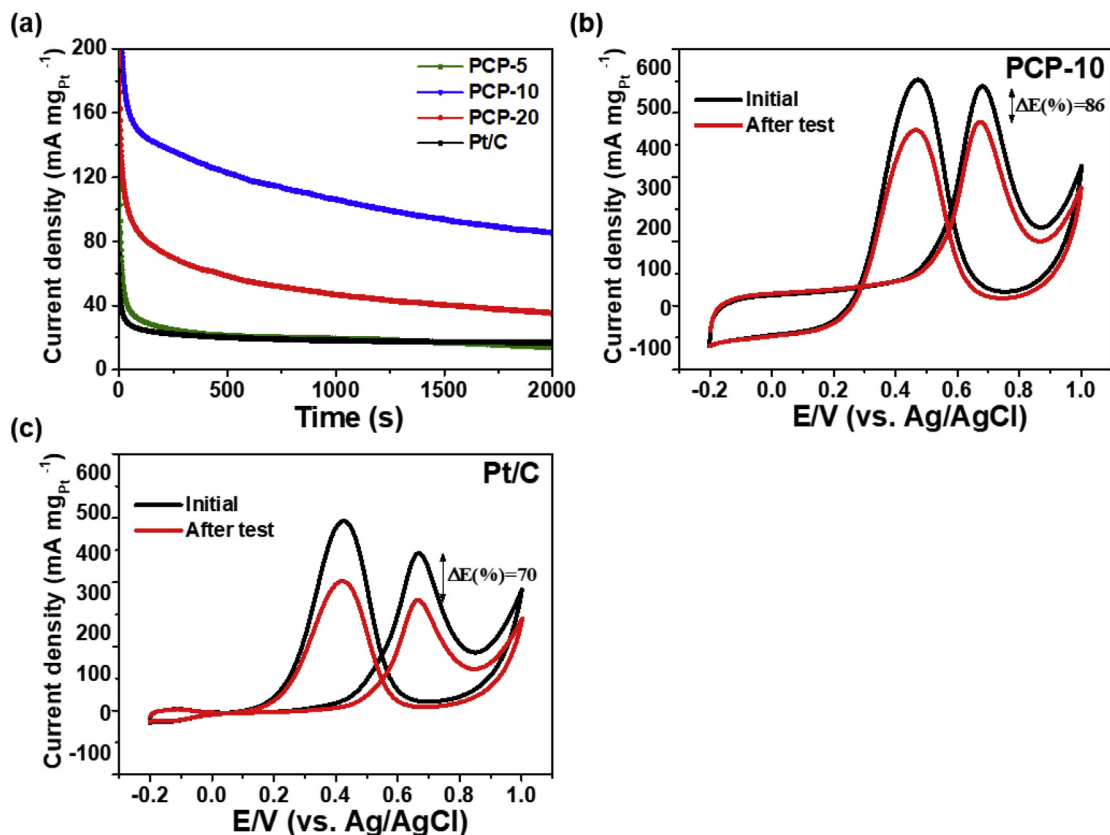


Fig. 6. (a) Chronoamperometry (CA) of PCP-5, PCP-10, PCP-20, and commercial Pt/C in electrolyte of 0.5 M H<sub>2</sub>SO<sub>4</sub> and 2 M CH<sub>3</sub>OH at 0.5 V, (b and c) CV measurements after CA test of PCP-10 and Pt/C, respectively.

potential of 0.07 V, the highest anodic current density of 510 mA  $\text{mg}_{\text{Pt}}^{-1}$ , excellent electrocatalytic stability with the highest retention rate of 86%. The excellent electrochemical performance of PCP-10 also became evident in terms of two major factors: (I) the improved anodic current density related to a good distribution of Pt electrocatalyst on the support; (II) the outstanding electrocatalytic stability related to the existence of N-doping in the support. Therefore, it can be concluded that this protein-based carbon is a promising candidate as a Pt electrocatalyst support, capable of offering a new strategy for high-performance DMFCs.

## Acknowledgments

This research was supported by Basic Science Research Program through the National Research Foundation of Korea funded by the Ministry of Science, ICT and Future Planning (NRF-2015R1A1A1A05001252).

## References

- [1] M.K. Debe, Electrocatalyst approaches and challenges, *Nature* 486 (2012) 43–51.
- [2] B.C.H. Steele, A. Heinzel, Materials for fuel-cell technologies, *Nature* 414 (2001) 345–352.
- [3] G.H. An, E.H. Lee, H.J. Ahn, Ruthenium and ruthenium oxide nanofiber supports for enhanced activity of platinum electrocatalysts in the methanol oxidation reaction, *Phys. Chem. Chem. Phys.* 18 (2016) 14859–14866.
- [4] X. Hu, C. Ge, N. Su, H. Huang, Y. Xu, J. Zhang, J. Shi, X. Shen, N. Satio, Solution plasma synthesis of Pt/ZnO/KB for photo-assisted electro-oxidation of methanol, *J. Alloys Compd.* 692 (2017) 848–854.
- [5] Y. Cheng, C. Xu, P.K. Shen, S.P. Jiang, Effect of nitrogen-containing functionalization on the electrocatalytic activity of PtRu nanoparticles supported on carbon nanotubes for direct methanol fuel cells, *Appl. Catal. B* 158–159 (2014) 140–149.
- [6] Y. Feng, J. Yang, H. Liu, F. Ye, J. Yang, Selective electrocatalysts toward a prototype of the membraneless direct methanol fuel cell, *Sci. Rep.* 4 (2014) 3813.
- [7] Z. Wang, C. Lu, W. Kong, Y. Zhang, J. Li, Platinum nanoparticles supported on core-shell niclecarbon as catalyst for methanol oxidation reaction, *J. Alloys Compd.* 690 (2017) 95–100.
- [8] G.H. An, H.J. Ahn, Pt electrocatalyst-loaded carbon nanofibre–Ru core–shell supports for improved methanol electrooxidation, *J. Electroanal. Chem.* 707 (2013) 74–77.
- [9] H. Huang, X. Hu, J. Zhang, N. Su, J.X. Cheng, Facile Fabrication of Platinum-Cobalt Alloy nanoparticles with enhanced electrocatalytic activity for a methanol oxidation reaction, *Sci. Rep.* 7 (2017) 45555.
- [10] K. Rokesh, A. Pandikumar, S.C. Mohan, K. Jothivenkatachalam, Aminosilicate sol-gel supported zinc oxide-silver nanocomposite material for photo-electrocatalytic oxidation of methanol, *J. Alloys Compd.* 680 (2016) 633–641.
- [11] S. Sharma, B.G. Pollet, Support materials for PEMFC and DMFC electrocatalysts—a review, *J. Power Sources* 208 (2012) 96–119.
- [12] B. Liu, H. Wang, Y. Chen, J. Wang, L. Peng, L. Li, Pt nanoparticles anchored on Nb<sub>2</sub>O<sub>5</sub> and carbon fibers as an enhanced performance catalyst for methanol oxidation, *J. Alloys Compd.* 682 (2016) 584–589.
- [13] G. Zhang, S. Sun, M. Cai, Y. Zhang, R. Li, X. Sun, Porous dendritic platinum nanotubes with extremely high activity and stability for oxygen reduction reaction, *Sci. Rep.* 3 (2013) 1526.
- [14] P.P. Patel, M.K. Datta, P.H. Jampani, D. Hong, J.A. Poston, A. Manivannan, P.N. Kumta, High performance and durable nanostructured TiN supported Pt<sub>50</sub>-Ru<sub>50</sub> anode catalyst for direct methanol fuel cell (DMFC), *J. Power Sources* 293 (2015) 437–446.
- [15] M.A. Alvi, M.S. Akhtar, An effective and low cost Pd-Ce bimetallic decorated carbon nanofibers as electro-catalyst for direct methanol fuel cells application, *J. Alloys Compd.* 684 (2016) 524–529.
- [16] J. Chang, L. Feng, C. Liu, W. Xing, X. Hu, Ni<sub>2</sub>P enhances the activity and durability of the Pt anode catalyst in direct methanol fuel cells, *Energy Environ. Sci.* 7 (2014) 1628–1632.
- [17] X. Li, M. Wen, D. Wu, Q. Wu, J. Li, Pd-on-NiCu nanosheets with enhanced electro-catalytic performances for methanol oxidation, *J. Alloys Compd.* 685 (2016) 42–49.
- [18] L. Wang, L. Zhao, P. Yu, C. Tian, F. Sun, H. Feng, W. Zhou, J. Wang, H. Fu, Silica direct approach to evaporation: a size-controlled SiC/carbon nanosheet composites as Pt catalyst supports for superior methanol electrooxidation, *J. Mater. Chem. A* 3 (2015) 24139–24147.
- [19] Q.L. Wang, R. Fang, L.L. He, J.J. Feng, J. Yuan, A.J. Wang, Bimetallic PdAu alloyed nanowires: rapid synthesis via oriented attachment growth and their high electrocatalytic activity for methanol oxidation reaction, *J. Alloys Compd.* 684 (2016) 379–388.
- [20] H. Huang, X. Wang, Recent progress materials for on carbon-based support electrocatalysts of direct methanol fuel cells, *J. Mater. Chem. A* 2 (2014) 6266–6291.
- [21] G.H. An, H.J. Ahn, Well-dispersed Pt catalysts supported on porous carbon nanofibers for improved methanol oxidation in direct methanol fuel cells, *ECS Solid State Lett.* 3 (2014) M29–M32.
- [22] H.L. An, G.H. An, H.J. Ahn, Octahedral Co<sub>3</sub>O<sub>4</sub>/carbon nanofiber composite-supported Pt catalysts for improved methanol electrooxidation, *J. Alloys Compd.* 645 (2015) 317–321.
- [23] D.Y. Lee, G.H. An, H.J. Ahn, High-surface-area tofu based activated porous carbon for electrical double-layer capacitors, *J. Ind. Eng. Chem.* 52 (2017) 121–127.
- [24] G.H. An, D.Y. Lee, H.J. Ahn, Tofu-derived carbon framework with embedded ultrasmall tin nanocrystals for high-performance energy storage devices, *J. Alloys Compd.* 722 (2017) 60–68.
- [25] T. Zhou, H. Wang, S. Ji, V. Linkov, R. Wang, Soybean-derived mesoporous carbon as an effective catalyst support for electrooxidation of methanol, *J. Power Sources* 248 (2014) 427–433.
- [26] F. Su, Z. Tian, C.K. Poh, Z. Wang, S.H. Lim, Z. Liu, J. Lin, Pt nanoparticles supported on nitrogen-coped porous carbon nanospheres as an electrocatalyst for fuel cells, *Chem. Mater.* 22 (2010) 832–839.
- [27] G.H. An, B.R. Koo, H.J. Ahn, Activated mesoporous carbon nanofibers fabricated using water etching-assisted templating for high-performance electrochemical capacitors, *Phys. Chem. Chem. Phys.* 18 (2016) 6587–6594.
- [28] G.H. An, D.Y. Lee, H.J. Ahn, Ultrafast lithium storage using antimony-doped tin oxide nanoparticles sandwiched between carbon nanofibers and a carbon skin, *ACS Appl. Mater. Interfaces* 8 (2016) 30264–30270.
- [29] G.H. An, E.H. Lee, H.J. Ahn, Well-dispersed iron nanoparticles exposed within nitrogen-doped mesoporous carbon nanofibers by hydrogen-activation for oxygen-reduction reaction, *J. Alloys Compd.* 682 (2016) 746–752.
- [30] J.N. Tiwari, R.N. Tiwari, G. Singh, K.S. Kim, Recent progress in the development of anode and cathode catalysts for direct methanol fuel cells, *Nanomater. Energy* 2 (2013) 553–578.
- [31] S. Zhao, H. Yin, L. Du, G. Yin, Z. Tang, S. Liu, Three dimensional N-doped graphene/PtRu nanoparticle hybrids as high performance anode for direct methanol fuel cells, *J. Mater. Chem. A* 2 (2014) 3719–3724.
- [32] A.R. Corpuz, T.S. Olson, P. Joghee, S. Pylypenko, A.A. Dameron, H.N. Dinh, K.J. O'Neill, K.E. Hurst, G. Bender, T. Gennett, B.S. Pivovar, R.M. Richards, R.P. O'Hayre, Effect of a nitrogen-doped Pt/Ru/carbon anode catalyst on the durability of a direct methanol fuel cell, *J. Power Sources* 217 (2012) 142–151.